An empirical prediction approach for seasonal fire risk in the boreal forests

Eden, J. M., Krikken, F. & Drobyshev, I.

Original citation & hyperlink:
Eden, JM, Krikken, F & Drobyshev, I 2020, 'An empirical prediction approach for seasonal fire risk in the boreal forests', International Journal of Climatology, vol. 40, no. 5, pp. 2732-2744.
https://dx.doi.org/10.1002/joc.6363

DOI 10.1002/joc.6363
ISSN 0899-8418
ESSN 1097-0088

Publisher: Wiley

An empirical prediction approach for seasonal fire risk in the boreal forests

Jonathan M. Eden

Centre for Agroecology, Water and Resilience (CAWR), Coventry University, UK.

Folmer Krikken

Royal Netherlands Meteorological Institute (KNMI), De Bilt, Netherlands.

Igor Drobyshev

Southern Swedish Forest Research Centre, Swedish University of Agricultural Sciences, Alnarp, Sweden

Universite du Quebec au Abitibi-Temiscamingue, Rouyn-Noranda, Canada

Abstract

The ability to predict forest fire risk at monthly, seasonal, and above-annual time scales is critical to mitigate its impacts, including fire-driven dynamics of ecosystem and socio-economic services. Fire is the primary driving factor of the ecosystem dynamics in the boreal forest, directly affecting global carbon balance and atmospheric concentrations of the trace gases including carbon dioxide. Resilience of the ocean-atmosphere system provides potential for advanced detection of upcoming fire season intensity.

Here, we report on the development of a probabilistic empirical prediction system for forest fire risk on monthly-to-seasonal timescales across the circumboreal region. Quasi-operational ensemble forecasts are generated for monthly drought code (MDC), an established indicator for seasonal fire activity in the Boreal biome based on monthly maximum temperature and precipitation values. Historical MDC forecasts are validated against observations, with good skill is found in across northern Eurasia and North America. In addition, we show that the MDC forecasts are an excellent indicator for satellite-derived observations of burned area in large parts of the Boreal region.

Our discussion considers the relative value of forecast information to a range of stakeholders when disseminated before and during the fire season. We also discuss the wider role of empirical predictions in benchmarking dynamical forecast systems and in conveying forecast information in a simple and digestible manner.

Key words: Forecasting (methods); Seasonal prediction; Forest fire; Empirical modelling.

1. Introduction

Wildfire constitutes an important natural hazard associated with a diverse set of environmental, social and economic impacts. The provision of forecast information about fire risk at monthly to seasonal timescales is critical to the mitigation of these impacts. Weather and climate play a key role in governing fire occurrence throughout the world (e.g. Flannigan et al., 2009); the extent to which fire risk may be predictable at these timescales is dependent on so-called teleconnections that describe the links between large-scale modes of variability in the climate system and local- or regional-scale anomalies. While seasonal climate forecasting is a regular service provided by many centres across the globe, the practice of forecasting fire risk at similar time scales is still relatively novel (e.g. Marcos et al., 2015; Bedía et al., 2018; Turco et al., 2018). As many forecasting efforts are often limited to specific regions there are large areas of the globe where the link of regional fire risk to large-scale climate, and therefore the potential for useful fire forecasts, is not yet clear. The boreal biome spanning Eurasia and North America is one of such regions.

Boreal fire activity accounts for approximately 12% of the total annual biomass burned globally (McRae et al., 2006) and is the main driving factor of ecosystem dynamics, directly affecting the global carbon balance in addition to atmospheric concentrations of carbon dioxide and other trace gases (Bond-Lamberty et al., 2007; Bowman et al., 2013). Changes in fire regimes impact significantly on forest composition, regeneration and growth conditions (Bergeron et al., 2004) and subsequently on carbon storage, biodiversity preservation and other ecosystem services (Bergeron et al., 2001; Bradshaw and Hannon, 2004; Adams, 2013). Additionally, the economies of local communities are dependent on the availability of forest products, including harvested softwood that accounts for 60% of the global total (Burton et al., 2010). Given that this region comprises one third of the world's forests and is potentially vulnerable to anthropogenic climate change, efforts to quantify the actual and potential limits of forecast skill is particularly important in understanding their usefulness for mitigation strategies.

Direct connections have previously been made between fire occurrence and sea surface temperature (SST) anomalies in the Pacific, Indian and Atlantic oceans during the preceding months (e.g. Chen et al., 2016; Drobyshev et al., 2019). However, the response of fire activity to such teleconnections is complex and inherently dependent on locally-varying factors (e.g. Moron et al., 2013). Additionally, calibration of forecast models of fire activity on historical fire records assumes that its dynamics are driven predominately by natural (climatic) factors. While the identification of regions with consistent fire-climate relationships is important, potentially of most use to stakeholders is the provision of a geographically-complete forecast alongside a clear indication of forecast skill, enabling the end user to interpret and act upon the forecast on a case-by-case basis. The use of global forecasts of seasonal climate, following both dynamical and empirical approaches, not only provides forecast information in a physically-consistent way but is also likely to be more applicable in a changing climate.

Dynamical (process-based) forecast systems continue to provide the most important platform for making predictions of seasonal climate at continental and regional scales. The numerical models that underpin such systems are able to, in principle, represent dynamical processes in and feedbacks between the atmosphere, ocean and land surface. The complexity of numerical climate models and the computational resources required to conduct the quantity of simulations necessary for reliable forecasting means that the development of dynamical systems is a continuous challenge (e.g. Doblas-Reyes et al., 2013). Even the most state-of-the-art models are associated with systematic errors and biases, with forecast skill severely limited in some regions of the globe. Empirical models, which seek to describe a known physical relationship between large-scale climate phenomena and local variations in a target variable, such as temperature or precipitation, can offer a credible alternative to their dynamical counterparts. Empirical models may range in complexity, from simply taking the value of a given variable at a given lead time as the forecast for the same variable (known as persistence) to analog- and regression-based methods that may in turn use sophisticated statistical techniques to decompose the predictive power of spatial patterns in climate fields.

Historically, application of empirical methods to seasonal forecasting has been done on an ad hoc basis, with focus given to a particular region or time scale. While this flexibility is a key benefit of empirical models in general, a global forecast system is required if the empirical approach is to either support or act as a credible alternative to dynamical forecast systems. To address this, Eden et al (2015) developed a prototype empirical system for generating probabilistic forecasts of temperature and precipitation across the globe. Since its development, monthly forecasts have been produced quasi-operationally and disseminated via the Royal Netherlands Meteorological Institute (KNMI) Climate Explorer (http://climexp.knmi.nl). In general, the empirical forecasts perform well in areas that are strongly teleconnected to well-known large-scale modes of variability in the climate system, including the El Nino Southern Oscillation (ENSO), the

Pacific Decadal Oscillation (PDO) and the Atlantic Multidecadal Oscillation (AMO). While there are regions and seasons for which empirical forecasts are not skilful, there are numerous examples during the quasi-operational phase where the empirical forecasts have been closer to observations than dynamical forecasts. The key benefit of empirical forecasts is the significantly lower computational complexity. By maximising this benefit there is considerable potential to generate forecasts for a variety of applications.

Here, we present an empirical approach to probabilistic prediction of monthly-to-seasonal forest fire risk in the circumboreal region. A variant of the empirical prediction system introduced by Eden et al. (2015) is used to generate ensemble forecasts of monthly drought code (MDC), an established indicator for seasonal fire activity in the Boreal biome based on maximum temperature and precipitation values (Girardin et al., 2009; van den Kamp et al., 2013). MDC forecasts are compared with corresponding observations of fire activity across North America and Eurasia, with correlation and probabilistic verification statistics used to identify regions of strong forecast performance. In the same way that empirical forecasts of seasonal climate provide a benchmark upon which to evaluate dynamical forecast products, the forecasts produced here may perform a similar role in respect to fire risk predictions produced by established forecast centres around the world.

Our analysis focuses first on the skill of the MDC forecasts across the circumboreal region. Secondly, we make comparisons between historical fire activity and corresponding MDC forecasts. In our conclusion we outline the benefits of such a system for the boreal region and other parts of the world.

2. Methods

2.1 Monthly Drought Code (MDC)

The MDC was developed by (Girardin and Wotton, 2009) as a monthly version of the Drought Code (DC), a daily moisture index used in forest management activities across Canada, northern Europe and northern Asia (de Groot et al., 2007). The DC is a simple approximation of the day-to-day changes in the moisture content of the deep organic layer derived from daily observations of maximum temperature, to estimate potential evapotranspiration, and cumulative precipitation. The DC may be used to characterise seasonal drought episodes but its derivation requires the availability of daily meteorological input data. Given that the relationships between the temperature and evapotranspiration and precipitation and soil moisture respectively are linear, Girardin and Wotton (2009) proposed a generalisation of the DC using monthly means. Both indices parameterise the moisture content of burnable organic matter. The MDC formulation, following Girardin and Wootton (2009), is summarised as follows. Potential evapotranspiration E_m during month *m* is given by:

$$E_m = N(0.36(\overline{T}_{\max}) + L_f$$

where $\overline{T}_{\max}$ is the monthly mean of daily maximum temperatures (°C) and *N* is the number of days in the month. The day adjustment factor L_f varies by month and represents the difference between noon and maximum temperature (van Wagner, 1987). The formulation assumes that total monthly precipitation occurs during the middle of the month and so first an estimation is made for the effect of precipitation on overall drying, $\mathrm{DC_{HALF}}$, calculated thus:

$$\mathrm{DC_{HALF}} = MDC_0 + 0.25E_m$$

where $\mathrm{MDC_0}$ is the MDC from the end of the previous month. The moisture equivalent Q_{mr} following precipitation is calculated:

$$Q_{mr} = 800e^{(-\frac{\mathrm{DC_{HALF}}}{400})} + 3.9397\mathrm{RM_{EFF}}$$

where $\mathrm{RM_{EFF}}$ is the effective precipitation, calculated by reducing total monthly rainfall r_m to account for canopy and surface interception ($\mathrm{RM_{EFF}} = 0.83r_m$). The estimate for MDC at the end of month *m* is given by:

$$\mathrm{MDC}_m = 400\ln\left(\frac{800}{Q_{mr}}\right) + 0.25E_m$$

The final MDC quantity is the average of the MDC values at the end of the current month MDC_m and previous month $\mathrm{MDC_0}$:

$$\mathrm{MDC} = (\mathrm{MDC_0} + \mathrm{MDC}_m)/2$$

The quantities expressed by both the MDC and Q_{mr} are unitless and there is no physical interpretation of the MDC value. Some experimental work indicates that DC values may be considered low when smaller than 200 and moderate when around 300 (e.g. de Groot et al., 2009; van der Kamp et al., 2013). Values greater than 400 are associated with the most intense burning (Girardin and Wotton, 2009). Such peaks tend to occur between mid-August and early September (van der Kamp, 2013).

2.2 Empirical forecasts

Some efforts have been made to forecast fire activity itself. Such an approach is complicated by the role of external factors in fire ignition, continuity and spread. This is particularly relevant at the local to regional scale. By contrast, in estimating fire risk indices such as MDC, it is possible to take forecasts of the constituent meteorological variables. As there is a degree of uncertainty with the forecast of each variable, this approach is potentially problematic for an index that relies on several variables. The MDC provides a robust solution as only two variables, maximum temperature and precipitation, are required thus reducing the cumulative forecast uncertainty.

Forecasts of maximum temperature and precipitation are taken from an established global empirical prediction system developed at the Royal Netherlands Meteorological Institute (KNMI). The system was designed with two purposes in mind: (a) to act as a benchmark for forecasts from dynamical systems, and (b) to serve as a forecast system in its own right. The system is used to generate monthly forecasts for the forthcoming three-month season which are then disseminated via the KNMI Climate Explorer. A detailed overview of the empirical prediction system and verification of its forecasts was given by Eden et al. (2015). Here, we provide a brief summary of the system and its application in the context of MDC forecasting.

The empirical prediction system is based on multiple linear regression and was designed to produce seasonal forecasts of temperature and precipitation using a number of predictors based on well-understood physical relationships. There is a growing acknowledgement that the temporal evolution of seasonal climate is governed not only by the internal variability of the climate system but also by the influence of anthropogenic climate change (Doblas-Reyes et al., 2013). A key component of the empirical prediction system was therefore to incorporate the long-term climate change signal as a source of skill. Additional predictors describing large scale modes of variability, including the El Nino Southern Oscillation (ENSO), local-scale information were included on the basis of their potential to add predictive power. The predictand time series x is therefore modelled as a function of a set of predictors thus:

$$x = \alpha + \beta C + \sum_{i=1}^{n} (\Phi_i F_i) + \epsilon$$

where C at a given lead time is the global CO_2 equivalent concentration a representation of the net forcing of greenhouse gases, aerosols and other anthropogenic emissions according to observations (until 2005) and the Representative Concentration Pathway (RCP) 4.5 (2005 onwards) (Meinshausen et al., 2011). F is a set of n additional predictors at the same lead time with regression parameters β and Φ required to transform C and F respectively. α is the constant regression parameter and ϵ is the set of residuals specific to the regression fit. An independent regression model is calibrated at each grid point and for each three-month season. Whereas *C* is always included as a predictor, the predictors in *F* are selected following a predictor selection procedure prior to model fitting.

The empirical prediction system uses a two-step predictor selection process to determine the fewest predictors necessary to provide greatest predictive power. The first step is undertaken prior to model fitting to determine which predictors exhibit good potential without collinearity with others. In a second step, predictors with potential are included in the model fitting. Again, a full description is given in (Eden et al., 2015).

Here, the same set of predictors used by Eden et al. (2015) to forecast mean temperature are used to forecast maximum temperature. These include a set of indices describing modes of variability in the climate system: NINO3.4 (which describes the phase and strength of ENSO), Pacific Decadal Oscillation (PDO), Atlantic Multidecadal Oscillation (AMO), Indian Ocean Dipole (IOD). Additionally, a set of locally-varying predictors are included: the previous month's value of the predictand, known as persistence (PERS), cumulative precipitation (CPREC) and the local sea surface temperature (LSST; defined as the average sea surface temperature in the five nearest-neighbour maritime gridcells). The relative contribution of each predictor, which differs both temporally and spatially, is very similar to that in the empirical models used to predict mean temperature; we direct the reader to Eden et al. (2015) for a full discussion. For summertime forecasts in the circumboreal region, the importance of NINO3.4 and PDO is limited at short lead times despite these being the most important predictors globally. AMO and IOD play a more important role in boreal Eurasia and both PERS and CPREC add considerable value in several regions. For precipitation, the same set of predictors agreed by Eden et al. (2015) are again used: NINO3.4, AMO, PERS and LSST. The relative contribution of NINO3.4 and AMO is strongest in North America and Eurasia respectively. Again, we direct the reader to Eden et al. (2015) for more detail.

The provision of probabilistic output was an important and novel component in the original system development and was achieved by randomly sampling the residuals ϵ of the original model fit. Whereas this has previously been done separately for each predictand, a key challenge here is to ensure a physical consistency between the two variables that will be used to calculate the MDC. To ensure a temporal alignment between residuals of temperature and precipitation, the residuals are therefore sampled in pairs.

2.3 Fire activity observations

In comparing historical forecasts with observations of fire activity, we first of all take monthly burned area data from the fourth version of the Global Fire Emissions Database (GFED), which contains estimates of monthly burned areas at 0.25° spatial resolution from mid-1995 to present. The GFED (van der Werf et al., 2006; 2010) is one of several global data sources of large-scale fire emissions based on satellite-derived fire activity and vegetation productivity information. Specifically, the fourth version (GFED4), which is fully described by Giglio et al. (2013), combines 500m MODIS maps of burned area with active fire data from the Along-Track Scanning Radiometer (ATSR) World Fire Atlas (Arino and Rosaz, 1999) and the Visible and Infrared Scanner (VIRS) (Giglio et al., 2003). GFED4 has been used regularly to link fire activity with large-scale modes of atmospheric-oceanic variability (e.g. Chen et al., 2016) and to verify forecasts of fire danger (Di Giuseppe et al., 2016). Secondly, we focus on specific large fires using data from the boreal burned area (BBA) dataset, a satellite-based fire scar product developed and described by Lehsten et al. (2014) that identifies spatiotemporal fire occurrence at daily timescales for the period 2001-2011. The BBA data is generated using several Moderate Resolution Imaging Spectroradiometer products with burned areas dated using thermal anomalies.

3. Results

3.1 MDC forecasts and verification

Efficiency of fire suppression relies, to a considerable degree, on the advance prediction of fire risk for the upcoming fire season in support of the optimal allocation of suppression resources over potentially vast geographic areas. Keeping this consideration in mind we use two prediction modes to generate MDC forecasts for each month in the northern hemisphere fire season (April to September). Mode 1 forecasts are generated during March for the entire fire season, and in doing so use a common predictor period of December-February. The three-month predictor period is consistent with that approach taken in the empirical prediction system's original development. Mode 2 forecasts are generated for each month independently at a one month lead time (e.g. the forecast for July is made during June using predictor data for March, April and May). Forecasts under the two modes are compared in order to understand, not only the degree of added value in updating forecasts each month, but also of the potential use of advance forecast information and the point at which the quality of that information may does not provide additional information relative to climatology.

Figure 1 shows the correlation between observed and forecasted MDC under modes 1 and 2 respectively for each month between 1961-2016. Correlation during April (for which the prediction period is identical in both prediction modes) is high across the Boreal zone, and greater than 0.6 in much of western Eurasia and eastern Canada. Under prediction mode 2, during May and June correlation generally remains similar across almost all of the Boreal zone, increasing slightly in July. August is associated with marginally stronger correlation in central and eastern Siberia. During September correlation is again stronger and up to 0.9 in parts of central Eurasia. Under prediction mode 1, correlation is sufficiently comparable to prediction mode 2 during May and June to suggest that skilful forecasts are possible at a lead time of up to three months and that subsequent planning activities would not benefit hugely from updated forecasts. During the later summer months, particularly August and September, forecast skill is far more dependent on a realistic representation of conditions throughout the earlier part of the fire season. For these months, the added value given by mode 2 in updating forecasts each month is clear. While the two-mode comparison is suitable for an analysis of the entire circumboreal region, the results suggest that forecast performance may be further improved at the regional scale by optimising lead times; for June in particular, skill in many areas is actually greater under the longer lead times in mode 1 than in mode 2.

3.2 Regional predictability of burned area

In this section, we explore the extent to which the MDC forecasts correspond with historical episodes of fire activity defined by burned area. We primarily use monthly burned areas values from the GFED4 dataset, described in Section 2.3. Burned area values are taken for each month at 1° x 1° resolution, which allows, in principle, for comparison between MDC and burned area to be made at each grid point throughout the Boreal domain. However, it is necessary to consider that fires are low frequency events, particularly when considering their occurrence within an area defined by a 1° x 1° grid box. In practice, the precise location of a fire event may not be so crucial to planning procedures and resource allocation. Rather, a forecast of anomalous fire risk within the proximity of an observed fire event may still constitute valuable forecast information (Di Giuseppe et al., 2016). Here, our forecast-fire activity comparison at a given point is made between spatial means of MDC and burned area within a 7° x 7° domain centred on the point of interest.

Firstly, we assess the degree of correspondence between observed MDC and burned area. MDC derived purely from contemporaneous observations has previously been shown to be strong predictor for burned area in the boreal region. For instance, van der Kamp et al. (2013) found MDC to be strongly correlated with regional burned area during the summer months (June-August) in southeast British Columbia (R_2 = 0.61). In an extension of this analysis across the circumboreal region, we consistently observed strong correlation ($r > 0.7$) throughout Eurasia and western and central Canada, particularly during June-August (not shown). From the perspective of seasonal prediction, the key question is, “Can we produce useful MDC forecasts up to several months in advance?” Figure 2 shows correlation between forecasted MDC and burned area from GFED4. Under mode 1, correlation > 0.5 during April is limited to the Russian far east; the general increase in fire activity during April is associated with correlations up to 0.6 in several parts of the North America and Eurasian sectors. Highest correlation is found during June ($r > 0.8$) and July ($r > 0.7$) in central

Eurasia. The performance of the MDC forecasts falls during August and September. Under mode 2, correlation patterns are broadly similar during April and May, suggesting there is little additional skill to be gained by updating forecasts each month. This situation begins to change from June when we observe correlation > 0.6 in more areas. During July and August, the performance is much improved under mode 2 in comparison to mode 1. High correlation during June persists into July and August, particularly in Siberia and the Russian far east. During September, for which there is minimal performance under mode 1, mode 2 forecasts produce correlation up to 0.9 in parts of eastern Siberia but offer little additional skill in western Eurasia.

It is clear that forecast mode 2 offers stronger performance overall, and particularly during the second half of the fire season. We therefore take mode 2 forecasts for use in subsequent analysis. However, we note that results for modes 1 and 2 are comparable during the April-June period, suggesting that it is possible to produce useful forecasts in advance of the entire first three months of the fire season across large parts of the circumboreal region. Only from July onwards do we see a marked benefit in running updated (mode 2) forecasts a month in advance.

Secondly, we seek to quantify forecast performance (mode 2) at the regional scale. To account for differences in the response of the natural environment to fire activity and consequent management strategies, our regional distinction is made between areas of land with broadly homogeneous vegetation and ecological characteristics within the boreal biome. These areas are defined by the World Wildlife Fund's Terrestrial Ecoregions of the World (TEOW) following Olson et al. (2001). Figure 3 details spatial means in observed and forecasted MDC for the full length fire season (April-September) alongside regionally-averaged burned area for a number of key ecoregions within the North American and Eurasian sectors of the wider circumboreal region. In boreal Eurasia, correlation between observed and forecasted MDC varies between 0.6 and 0.9 across most zones and is strongest in the Siberian ecoregions. Only in the West Siberian taiga region do we find a significant relationship between forecasted MDC and burned area ($r = 0.40$); increased fire activity during the 2001, 2006 and, particularly, 2013 seasons is associated with MDC anomalies that are well-captured by the forecasts. In boreal North America, correlation between ecoregion observed and forecasted MDC is consistently high ($r > 0.7$). In the Mid-Continental Canadian forests, where we observe a significant correlation ($r = 0.41$) between ecoregion-specific MDC and burned area, we again find that years with regionally increased fire activity (1999, 2003, 2011 and 2016) correspond with forecasts of anomalous MDC value ($r = 0.41$). There is less consistency across the other North American ecoregions but still some evidence that years of greatest burning are associated with forecasts of above-average MDC values (e.g. during 1999 and 2005 in the Muskwa-Slave Lake forests zone).

In general, the MDC forecasts show decent potential as a predictive tool for fire risk in large parts of the circumboreal region, particularly when updated at one-month lead times throughout the fire season. In some areas, strong forecast performance is consistent with previous work showing a high degree of predictability on the basis of established teleconnections. This includes, for instance, the link between ENSO-related SST anomalies and fire activity in north-east Eurasia (Chen et al., 2016). Key to the findings presented here are the examples of predictive skill in other parts of Eurasia and North America that have not previously been identified.

3.3 Forecasts and individual fires

We now assess the capacity of the MDC forecasts to predict increased fire risk coinciding with large fires. In other words, to what extent can the empirical prediction system have been used to predict the occurrence of the largest circumboreal fires during a particular historical period? Here, we use the BBA dataset (Lehsten et al., 2014) with detailed information on the location, timing and duration of individual fires for the period 2001-2011. We focus on the largest 10% of fires (defined by estimated burned area) only. Figure 4 illustrates the spatial distribution of this set of fires, again during the six component months of the fire season. Each fire episode is compared with the corresponding MDC forecast for the same location, month and year. As expected, the largest fires are associated with anomalous MDC forecasts; in many areas, the forecast falls above the observed 75th percentile. These include large parts of eastern and central Eurasia and, between May and July, the boreal forests of northern Europe. In North America, the majority of corresponding forecasts are above the 50th percentile but there are fewer above the 75th percentile. Likewise, September fires across Eurasia are rarely associated with strongly anomalous MDC forecasts.

Figure 4 provides clear evidence that historical MDC forecasts may have been useful as a predictive tool for circumboreal fire risk during the study period, particularly in the Eurasian sector. Our focus now shifts to the peak-summer months (June-August) and to the largest and most damaging individual fires. The MDC forecasts for this period show greatest overall skill as a predictor for burned area (Figure 2b). Peak-summer fires associated with burned areas larger than 500 ha are categorised into three levels of severity: 500-1000 ha, 1000-2000 ha and > 2000 ha. Figure 5 details the spatial distribution of fire episodes in these three categories and the associated MDC forecast. Large fire years throughout eastern Eurasia were associated with values above 300; by contrast, the largest fires in North American are rarely associated with MDC forecasts that exceed 200. We present MDC values as anomalies with respect to the climatology given the substantial regional variation exhibited. MDC forecasts fall above the climatological 75th percentile in 60-70% of cases. However, it would be dangerous to place faith in MDC forecasts without considering regional variation in skill.

The largest circumboreal fire episodes are found to be frequently associated with anomalous MDC values, suggesting that such forecasts have the potential to correctly inform fire management authorities of increased likelihood of fire activity. However, as the MDC forecasts clearly do not resolve sub-monthly variations that facilitate fire spread, the largest fires are not always linked to the highest MDC values. While this forecast approach has the capacity to provide information to support the distribution of resources, additional information from meteorological (i.e. daily) forecasts is required to explicitly predict fire severity.

4. Discussion and outlook

The links between fire risk and the natural variability of the atmosphere-ocean system, while complex, are a pathway to predictability. Many studies have previously explored patterns in area burned by fire activity and the relationship with, for instance, global SST anomalies (e.g. Chen et al., 2016). In general, areas of significant fire-SST relationships are limited to regions where temperature and precipitation exhibit strong teleconnections with ENSO, PDO and other modes of variability. Outside the tropics, such teleconnections are not as persistent, leaving us with large gaps in our understanding of fire-climate relationships, potential for predictability and development of early warning systems. The boreal region, with a third of the world's forested area, is one such gap where an improved understanding and forecasting capabilities is potentially very useful to fire management strategies.

Here, the capacity for monthly-to-seasonal prediction of circumboreal fire risk has been assessed using an empirical prediction system built to the fullest extent on physical principles. Monthly drought code (MDC), an established metric for meteorological conditions conducive to the spread and prevalence of circumboreal fires, was derived from forecasts of maximum temperature and precipitation using predictor information from a variety of climate indices. We found, first of all, that MDC estimates derived from empirical forecasts compare favourably with those derived from observations in large parts of the circumboreal region, particularly when generated no more than a month in advance. Secondly, we found MDC forecasts to be a reliable indicator for burned area metrics in large parts of the circumboreal region. This included areas where there exists little prior evidence of strong relationship between fire risk and modes of variability within the climate system.

These results are sufficiently encouraging to suggest scope for the empirical system to act, not only as a benchmark to judge the effectiveness of dynamical forecast system based on numerical models, but also as a forecast tool in its own right. Concerning the second purpose, it is important to consider the limitations of dynamical forecast systems and where an empirical approach may add value. In general, strong performance in dynamical forecasts is limited to regions of the tropics where well-established teleconnections are captured by the underpinning numerical models. Outside these regions, and particularly in the globe's northern latitudes, the random variability of the climate system exerts a far greater governance on seasonal variations in temperature and precipitation (Kumar et al., 2007; Arribas et al., 2011). The empirical forecasts produced here are sufficiently promising to act both as a benchmarking tool and, crucially, as a supplement to dynamical forecasts.

As discussed in the introduction, the practice of predicting seasonal fire risk is still in its infancy and further development should seek to expand on existing approaches to forecasting on shorter timescales. We recognise that the DC, for which the MDC is an extension, is just one component of the Fire Weather Index (FWI), a metric widely-used to estimate fire risk. The DC, and consequently the MDC, do not include a quantification of wind speed, which is considered a major control on fire spread. Our results show generally high predictive skill despite the omission of wind, possibly due to the association of large fires with the persistent blocking episodes common to much of the study region during the summer months. But the adaptation of the FWI and other wind-inclusive indices from daily to seasonal timescales may add value to overall forecast skill, particularly outside the circumboreal region. In addition, such adaptation is likely to support the complementarity of forecasts on different timescales in order to prepare for and explicitly predict fire activity.

Research into understanding and predicting present and future changes in wildfire activity is an expanding subfield that bridges the climate, biological and social sciences. The true test of any forecast product with regard to its usefulness is to facilitate its application to real world scenarios. It is intended for the forecast system presented here to be implemented in a quasi-operational framework. Alongside the existing set of forecasts and verification metrics, monthly MDC forecasts for the circumboreal region will be generated and publicly disseminated via the KNMI Climate Explorer. We anticipate that future development of the forecast system will be supported by two-way dialogue with forest management authorities and other relevant stakeholders.

Acknowledgements

This research leading to these results received funding from the Belmont Forum under the PREREAL project.

References

Adams MA (2013) Mega-fires, tipping points and ecosystem services: Managing forests and woodlands in an uncertain future. *Forest Ecology and Management,* **294,** 250-261.

Arribas, A., Glover, M., Maidens, A., Peterson, K., Gordon, M., MacLachlan, C., Graham, R., Fereday, D., Camp, J., Scaife, A. A., Xavier, P., McLean, P., Colman, A., and Cusack, S. : The GloSea4 ensemble prediction system for seasonal forecasting, Mon. Weather Rev., 139, 1891–1910, 2011.

Bedía, J., Golding, N., Casanueva, A., Iturbide, M., Buontempo, C. and Gutiérrez., J.M. (2018) Seasonal predictions of Fire Weather Index: Paving the way for their operational applicability in Mediterranean Europe, *Clim. Serv.*, 9, 101-110.

Bergeron Y, Flannigan M, Gauthier S, Leduc A, Lefort P (2004) Past, current and future fire frequency in the Canadian boreal forest: Implications for sustainable forest management. *Ambio,* **33,** 356-360.

Bond-Lamberty B, Peckham SD, Ahl DE, Gower ST (2007) Fire as the dominant driver of central Canadian boreal forest carbon balance. *Nature,* **450,** 89-92.

Bowman DM, Murphy BP, Boer MM, et al (2013) Forest fire management, climate change, and the risk of catastrophic carbon losses. *Frontiers in Ecology and the Environment,* **11,** 66-68.

Bradshaw RHW, Hannon GE (2004) The holocene structure of north-west European temperate forest induced from palaeoecological data. *Forest Biodiversity: Lessons from History for Conservation,* **10,** 11-25.

Burton PJ, Bergeron Y, Bogdansky BEC, et al (2010) Sustainability of boreal forests and forestry in a changing environment. In:*Forests and society – responding to global drivers of change* (eds Mery G, Katila P, Galloway G, Alfaro R, Kanninen M, Lobovikov M, Varjo J), pp. 249-282. IUFRO.

Chen, Y., Morton, D.C., Andela, N., Giglio, L. and Randerson, J.T. (2016) How much global burned area can be forecast on seasonal time scales using sea surface temperatures? Env. Res. Lett. 11 045001.

de Groot WJ, Field RD, Brady MA, Roswintiarti O, Mohamad M (2007a) Development of the Indonesian and Malaysian Fire Danger Rating Systems. Mitigation and Adaptation Strategies for Global Change, 12, 165–180.

de Groot WJ, Landry R, Kurz WA et al. (2007b) Estimating direct carbon emissions from Canadian wildland fires. International Journal of Wildland Fire, 16, 593–606.

Di Giuseppe, F., Pappenberger, F., Wetterhall, F., Krzeminski, B., Camia, A., Libertá, G. and San Miguel, J. (2016) The Potential Predictability of Fire Danger Provided by Numerical Weather Prediction, *J. Appl. Meteor. Climatol.,* **55**, 2469–2491

Doblas-Reyes FJ, Garcia-Serrano J, Lienert F, Biescas AP, Rodrigues LRL (2013) Seasonal climate predictability and forecasting: status and prospects. *Wiley Interdisciplinary Reviews- Climate Change*, **4,** 245-268.

Drobyshev, I., Bergeron, Y., de Vernal, A., Moberg., A., Ali., A.A. and Niklasson, M. (2016) Atlantic SSTs control regime shifts in forest fire activity of Northern Scandinavia, Sci. Rep., 6, 22532.

Eden JM, van Oldenborgh GJ, Hawkins E, Suckling EB (2015) A global empirical system for probabilistic seasonal climate prediction. *Geosci. Model Dev*., **8,** 3941-3970.

Flannigan MD, Krawchuk MA, de Groot WJ, Wotton BM, Gowman LM (2009) Implications of changing climate for global wildland fire. *International Journal of Wildland Fire*, **18,** 483-507.

Girardin, M.P., Ali, A.A., Carcaillet, C. Mudelsees,M., Drobyshev, I., Hély, C. and Bergeron, Y. (2009) Heterogeneous response of circumboreal wildfire risk to climate change since the early 1900s, *Global Change Biology*, 15, 2751-2769.

Girardin, M.P. and Wotton, B.M. (2009) Summer moisture and wildfire risks across Canada, *Journal of Applied Meteorology and Climatology*, 48, 517-533.

Kumar, A., Jha, B., Zhang, Q., and Bounoua, L.: A new methodology for estimating the unpredictable component of seasonal atmospheric variability, J. Climate, 20, 3888–3901, 2007.

Lehsten, V., W. J. de Groot, M. Flannigan, C. George, P. Harmand, and H. Balzter (2014), Wildfires in boreal ecoregions: Evaluating the power law assumption and intra‐annual and interannual variations, *J. Geophys. Res. Biogeosci.*, 119, 14–23.

Marcos, R., Turco, M., Bedía, J., Llasat, M.C. and Provenzale, D. (2015) Seasonal predictability of summer fires in a Mediterranean environment, *Int. J. Wildland Fire*, 24, 1076-1084.

McRae D, Conard S, Ivanova G, et al (2006) Variability of fire behavior, fire effects, and emissions in Scotch pine forests of Central Siberia. *Mitigation and Adaptation Strategies for Global Change*, **11,** 45-74.

Moron, V., R. Barbero, M. Mangeas, L. Borgniet, T. Curt, and L. Berti-Equille, 2013: Prediction of September–December Fire in New Caledonia (Southwestern Pacific) Using July Niño-4 Sea Surface Temperature Index. J. Appl. Meteor. Climatol., 52, 623–633.

Meinshausen, M., Smith, S. J., Calvin, K., Daniel, J. S., Kainuma, M. L. T., Lamarque, J.-F., Matsumoto, K., Montzka, S. A., Raper, S. C. B., Riahi, K., Thomson, A., Velders, G. J. M., and van Vuuren, D. P. P. (2011) The RCP greenhouse gas concentrations and their extensions from 1765 to 2300, Climatic Change, 109, 213–241.

Olson, D. M., Dinerstein, E., Wikramanayake, E. D., Burgess, N. D., Powell, G. V. N., Underwood, E. C., D'Amico, J. A., Itoua, I., Strand, H. E., Morrison, J. C., Loucks, C. J., Allnutt, T. F., Ricketts, T. H., Kura, Y., Lamoreux, J. F., Wettengel, W. W., Hedao, P., Kassem, K. R. (2001). Terrestrial ecoregions of the world: a new map of life on Earth, Bioscience, 51 (11), 933-938.

Turco, M., Jerez, S., Doblas-Reyes., F.J., AghaKouchak, A., Llasat, M.C., Provenzale, A. (2018) Skilful forecasting of global fire activity using seasonal climate predictions, Nat. Commun., 9:2718.

van der Kamp, D.W., Bürger, G. and Werner, A.T. (2013) Evaluation of the monthly drought code as a metric for fire weather in a region of complex terrain, and uncertainties in future projections. The Pacific Climate Impacts Consortium, Victoria, British Columbia, Canada.

Figure 1: Correlation of (a) mode 1 and (b) mode 2 empirical forecast-derived MDC with observation-derived MDC within the circumboreal region for April to September (1961-2016).

Figure 2: Correlation of (a) mode 1 and (b) mode 2 empirical forecast-derived MDC with GFED-derived average area burned within the circumboreal region for April to September (1996-2016).

Figure 3: Spatial mean observed (black) and mode 2 forecasted (green) MDC (1961-2016) alongside average area burned per month per month (AAB; red; 1996-2016) in eight homogenous terrestrial ecosystems across the circumboreal region. Means calculated for April-September. Correlation (and p value) between observed and forecasted MDC shown in top left corner of each panel (black); correlation (and p value) between forecasted MDC and observed burned area shown in bottom left corner of each panel (red).

Figure 4: Spatial and intra-seasonal distribution of the largest 10% of observed fires (in terms of area burned) between 2000-2011 and the magnitude of each corresponding MDC forecast; colour at each point illustrates the MDC forecast terms of which quartile it falls each into (e.g. Q4 is the case when the forecast is above the historical 75th percentile at that particular location).

Figure 5: Spatial distribution of fires associated with a total burned area larger than 500 hectares; the size and colour of the bubble indicates the size of the burned area and the corresponding MDC forecast respectively. The lower-left insert in each panel indicates the proportion of MDC forecasts falling in one of four quartiles during a fire occurrence.

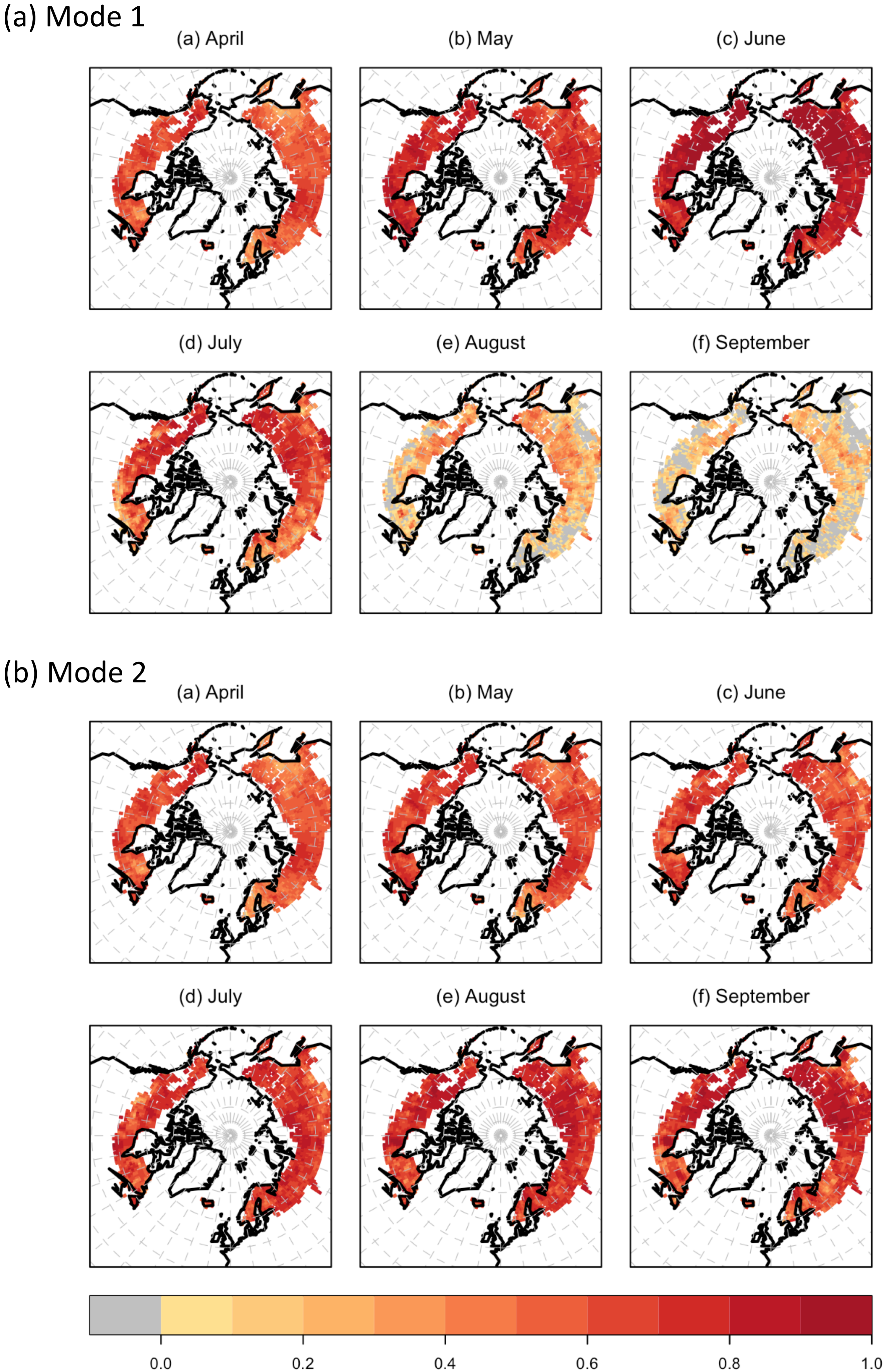
(a) Mode 1
(a) April
(b) May
(c) June
(d) July
(e) August
(f) September
(b) Mode 2
(a) April
(b) May
(c) June
(d) July
(e) August
(f) September
0.0
0.2
0.4
0.6
0.8
1.0

Figure 1: Correlation of (a) mode 1 and (b) mode 2 empirical forecast-derived MDC with observation-derived MDC within the circumboreal region for April to September (1961-2016).

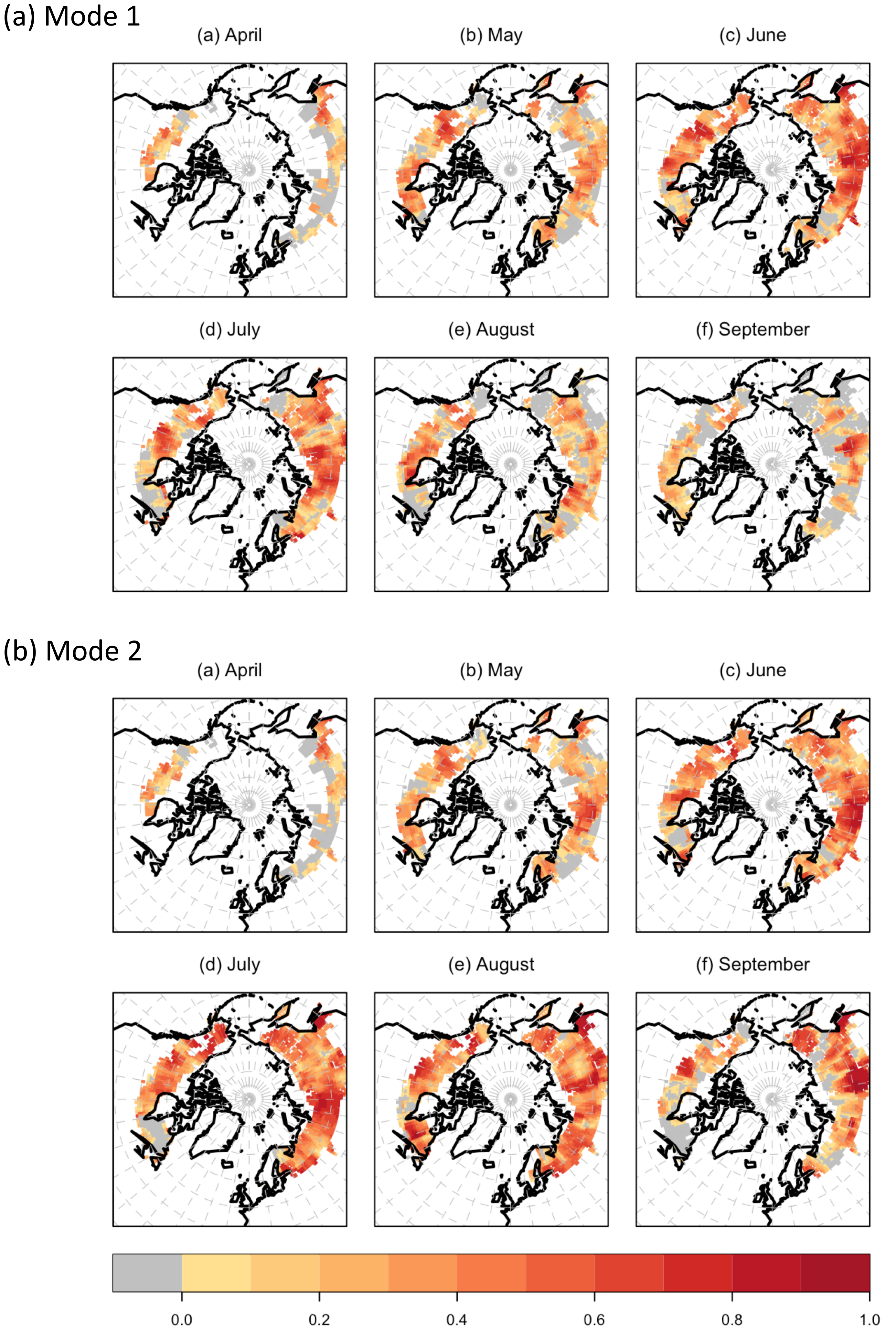
(a) Mode 1
(a) April
(b) May
(c) June
(d) July
(e) August
(f) September
(b) Mode 2
(a) April
(b) May
(c) June
(d) July
(e) August
(f) September
0.0
0.2
0.4
0.6
0.8
1.0

Figure 2: Correlation of (a) mode 1 and (b) mode 2 empirical forecast-derived MDC with GFED-derived average area burned within the circumboreal region for April to September (1996-2016).

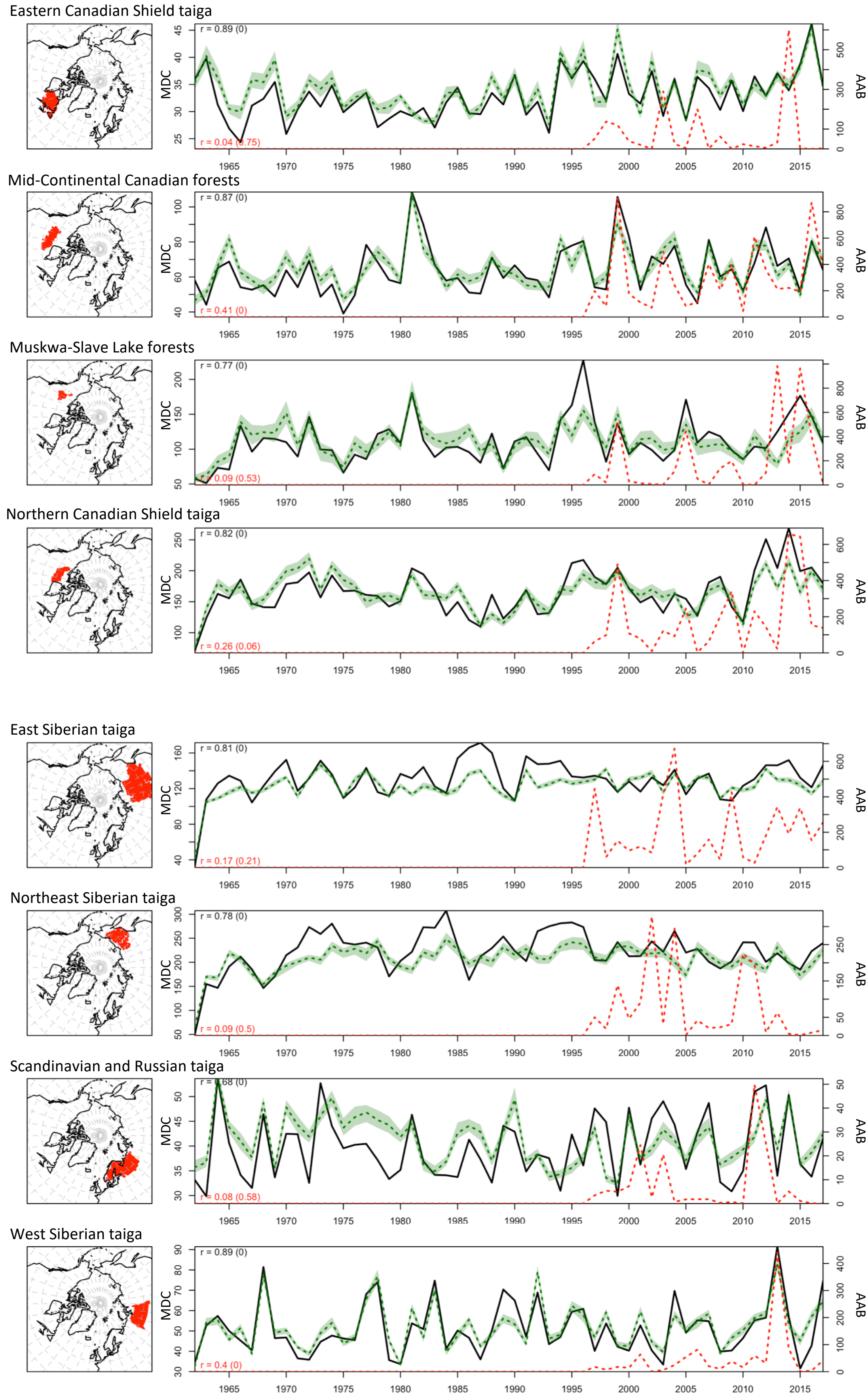

Eastern Canadian Shield taiga
r = 0.89 (0)
r = 0.04 (0.75)
Mid-Continental Canadian forests
r = 0.87 (0)
r = 0.41 (0)
Muskwa-Slave Lake forests
r = 0.77 (0)
r = 0.09 (0.53)
Northern Canadian Shield taiga
r = 0.82 (0)
r = 0.26 (0.06)
East Siberian taiga
r = 0.81 (0)
r = 0.17 (0.21)
Northeast Siberian taiga
r = 0.78 (0)
r = 0.09 (0.5)
Scandinavian and Russian taiga
r = 0.08 (0.58)
West Siberian taiga
r = 0.89 (0)
r = 0.4 (0)
MDC
AAB

Figure 3: Spatial mean observed (black) and mode 2 forecasted (green) MDC (1961-2016) alongside average area burned (AAB; red; 1996-2016) in eight homogenous terrestrial ecosystems across the circumboreal region. Correlation (and p value) between observed and forecasted MDC shown in top left corner of each panel (black); correlation (and p value) between forecasted MDC and observed AAB shown in bottom left corner of each panel (red).

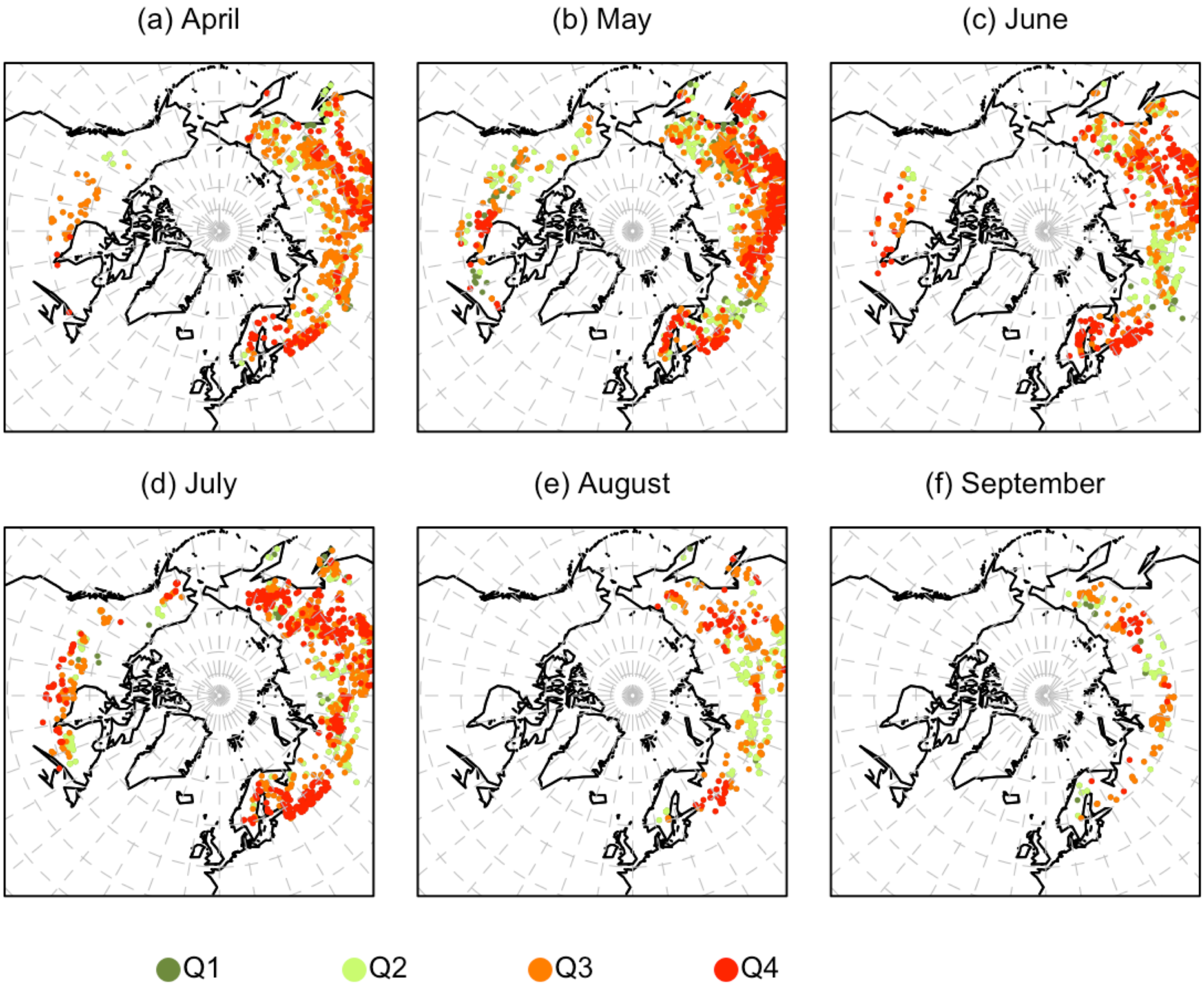
(a) April
(b) May
(c) June
(d) July
(e) August
(f) September
Q1
Q2
Q3
Q4

Figure 4: Spatial and intra-seasonal distribution of the largest 10% of observed fires (in terms of area burned) between 2000-2011 and the magnitude of each corresponding MDC forecast; colour at each point illustrates the MDC forecast terms of which quartile it falls each into (e.g. Q4 is the case when the forecast is above the historical 75th percentile at that particular location).

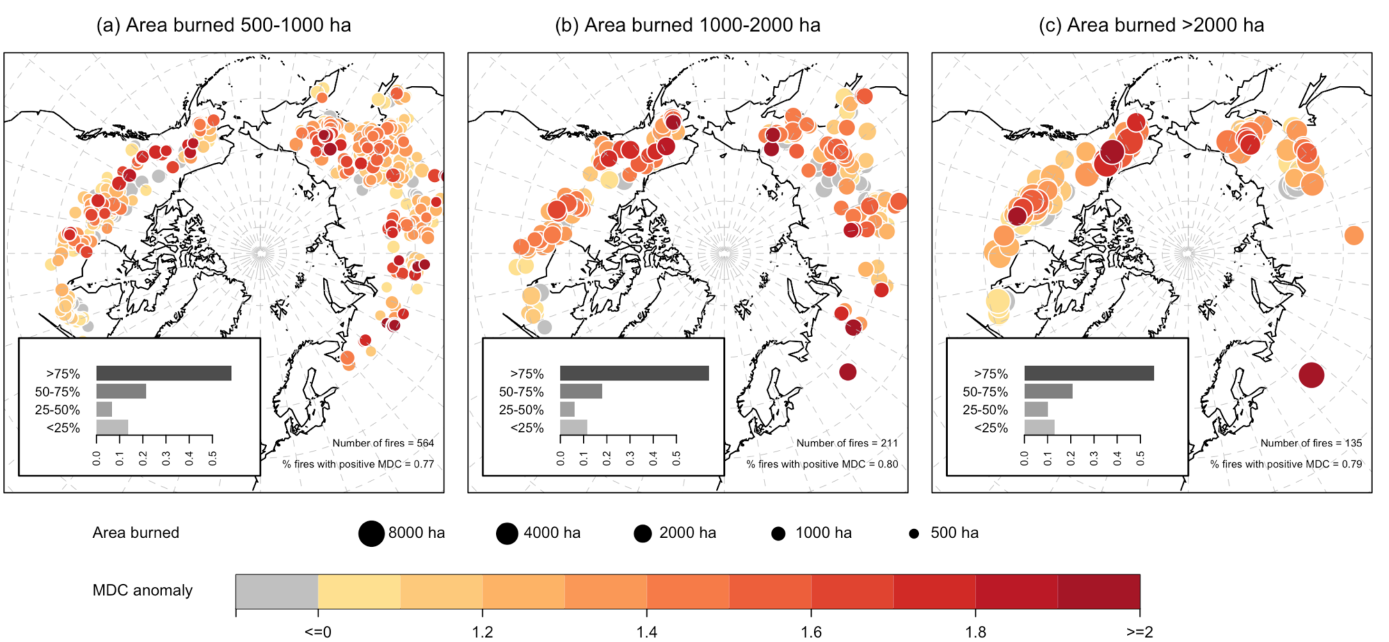

(a) Area burned 500-1000 ha
(b) Area burned 1000-2000 ha
(c) Area burned >2000 ha
>75%
50-75%
25-50%
<25%
0.0 0.1 0.2 0.3 0.4 0.5
Number of fires = 564
% fires with positive MDC = 0.77
Number of fires = 211
% fires with positive MDC = 0.80
Number of fires = 135
% fires with positive MDC = 0.79
Area burned
8000 ha
4000 ha
2000 ha
1000 ha
500 ha
MDC anomaly
<=0
1.2
1.4
1.6
1.8
>=2

Figure 5: Spatial distribution of fires associated with a total burned area larger than 500 hectares; the size and colour of the bubble indicates the size of the burned area and the corresponding MDC forecast respectively.